Continuous blade coating for multi-layer large-area organic light-emitting diode and solar cell

Chun-Yu Chen, Hao-Wen Chang, Yu-Fan Chang, Bo-Jie Chang, Yuan-Sheng Lin, Pei-Siou Jian, Han-Cheng Yeh, Hung-Ta Chien, En-Chen Chen, Yu-Chiang Chao, Hsin-Fei Meng, Hsiao-Wen Zan, Hao-Wu Lin, Sheng-Fu Horng, Yen-Ju Cheng, Feng-Wen Yen, I-Feng Lin, Hsiu-Yuan Yang, Kuo-Jui Huang, and Mei-Rurng Tseng

Citation: Journal of Applied Physics **110**, 094501 (2011); doi: 10.1063/1.3636398
View online: http://dx.doi.org/10.1063/1.3636398
View Table of Contents: http://scitation.aip.org/content/aip/journal/jap/110/9?ver=pdfcov
Published by the AIP Publishing

Continuous blade coating for multi-layer large-area organic light-emitting diode and solar cell

Chun-Yu Chen,[1] Hao-Wen Chang,[2] Yu-Fan Chang,[3] Bo-Jie Chang,[2] Yuan-Sheng Lin,[3] Pei-Siou Jian,[4] Han-Cheng Yeh,[5] Hung-Ta Chien,[6] En-Chen Chen,[2] Yu-Chiang Chao,[1] Hsin-Fei Meng,[1,a)] Hsiao-Wen Zan,[7] Hao-Wu Lin,[8] Sheng-Fu Horng,[2] Yen-Ju Cheng,[9] Feng-Wen Yen,[10] I-Feng Lin,[10] Hsiu-Yuan Yang,[11] Kuo-Jui Huang,[11] and Mei-Rurng Tseng[12]

[1]*Institute of Physics, National Chiao Tung University, Hsinchu 300, Taiwan*
[2]*Department of Electrical Engineering, National Tsing Hua University, Hsinchu 300, Taiwan*
[3]*Institute of Photonics Technologies, National Tsing Hua University, Hsinchu 300, Taiwan*
[4]*Institute of Lighting and Energy Photonics, National Chiao Tung University, Hsinchu 300, Taiwan*
[5]*Institute of Electro-Optical Engineering, National Chiao Tung University, Hsinchu 300, Taiwan*
[6]*Department of Electrophysics, National Chiao Tung University, Hsinchu 300, Taiwan*
[7]*Department of Photonics, National Chiao Tung University, Hsinchu 300, Taiwan*
[8]*Department of Materials Science and Engineering, National Tsing Hua University, Hsinchu 300, Taiwan*
[9]*Department of Applied Chemistry, National Chiao Tung University, Hsinchu 300, Taiwan*
[10]*Luminescence Technology Corporation, Hsinchu 300, Taiwan*
[11]*Flash Innovation Company Limited, Hsinchu 304, Taiwan*
[12]*Material and Chemical Research Laboratories, Industrial Technology Research Institute, Hsinchu 310, Taiwan*

(Received 11 May 2011; accepted 6 August 2011; published online 2 November 2011)

A continuous roll-to-roll compatible blade-coating method for multi-layers of general organic semiconductors is developed. Dissolution of the underlying film during coating is prevented by simultaneously applying heating from the bottom and gentle hot wind from the top. The solvent is immediately expelled and reflow inhibited. This method succeeds for polymers and small molecules. Uniformity is within 10% for 5 cm by 5 cm area with a mean value of tens of nanometers for both organic light-emitting diode (OLED) and solar cell structure with little material waste. For phosphorescent OLED 25 cd/A is achieved for green, 15 cd/A for orange, and 8 cd/A for blue. For fluorescent OLED 4.3 cd/A is achieved for blue, 9 cd/A for orange, and 6.9 cd/A for white. For OLED with 2 cm by 3 cm active area, the luminance variation is within 10%. Power conversion efficiency of 4.1% is achieved for polymer solar cell, similar to spin coating using the same materials. Very-low-cost and high-throughput fabrication of efficient organic devices is realized by the continuous blade-only method. © *2011 American Institute of Physics*. [doi:10.1063/1.3636398]

I. INTRODUCTION

As a unique form of light source, organic light-emitting diode (OLED) offers several remarkable advantages including thin thickness, large area with potential flexibility, warm color, and environmental-friendly production. OLED is now considered an emerging technology for lighting as well flat-panel display. The standard architecture of an OLED has a multi-layer structure.[1–8] In addition to the emissive layer, the transport layers help the carriers to overcome the high energy barrier between the electrodes and the emissive layer. The carrier blocking layers often also act as the blocking layers to confine the carriers in the emissive layer for recombination. High band gap exciton layers are needed to prevent the energy transfer to the transport layers for blue emission. Doped transport layers next to the electrode may form Ohmic contact and reduce the operation voltage. Through the implementation of the device physics concept in the multi-layer design, efficiency much higher than the incandescent lamp and comparable to the fluorescent lamp is achieved in multi-layer structures fabricated by successive thin film deposition by thermal evaporation in high vacuum.[9] The cost for such vacuum deposition is, however, intrinsically high due the following reasons. The vacuum system itself for large size has a high cost; the majority of the organic semiconductors is deposited onto the chamber wall and wasted; the pumping time limits the throughput; and finally co-evaporation of host-guest layer requires accurate ratio and limits the reproducibility. Solution deposition of organic semiconductors with very low production cost is, therefore, necessary to make OLED widely applied in the daily life. However, to satisfy the general requirement for high efficiency and easy production, the solution deposition method has to meet a few conditions. First, it needs to allow multi-layer depositions of organic semiconductors with similar solvents. Second, the material waste needs to be low. Third, it should be a continuous process, with the potential of roll-to-roll deposition. Unfortunately, so far most of the common solution deposition methods do not satisfy all of the

a)Author to whom correspondence should be addressed. Electronic mail: meng@mail.nctu.edu.tw.

three conditions. Spin-coating gives large uniform films, but it cannot be used for multi-layer deposition because of the mutual dissolution. Besides in general, only about 5% of the materials are left on the substrate and the rest of them wasted. Inkjet printing has low material waste and good patterning resolution, but it cannot make multi-layer structure due to dissolution and has mechanical complications at the printer head. Slot die coating can deposit large and uniform film, but there is no report on multi-layer coating. Furthermore, it is a large and complicated system incompatible with the common nitrogen glove box. The delivery system requires a large amount of solution in the order of a liter to operate.

Recently, a blade coating method is developed to deposit multi-layer of organic semiconductors in solution.[10–15] Dissolution problem faced by other solution deposition methods is avoided by the concurrence of two factors. First, the wet film, rapidly deposited by a fast-moving blade, on top of the dry film underneath is only ten of micrometers in thickness and contains a small amount of solvent. Second, before the dissolution of the underlying dry film, to occur in a few seconds, the solvent of the second layer is rapidly expelled. In the previous reports, rapid drying of the wet film is achieved by a spinning after blade coating. The horizontal gas flow circulating around the substrate during spinning is efficient to realize drying in a few seconds. The centrifugal force of spinning also ensures horizontal uniformity in case of a small level of dissolution. Note that the majority of the materials remain on the substrate during spinning of the thin wet film. Such deposition is termed blade-spin. Multi-layers of organic semiconductors can be deposited by the blade-spin method for large area with low material waste. Device efficiency comparable to vacuum deposition is achieved by this method.[11] The major problem for blade-spin is that it is not a continuous process. The spinning restricts the fabrication to be piece-by-piece and severely limits the throughput. Spinning is also incompatible with the ultimate roll-to-roll process.

In this paper, we present a new version of blade coating termed blade-only method in which multi-layer of organic films are deposited in large-area without the limiting spinning step. Hot wind from the top is crucial to its success. As discussed above, rapid drying of the wet film is the key to prevent dissolution. Without the circulating gas flow during spinning, one nature way to enforce rapid drying is substrate heating. There is, however, a dilemma for substrate heating. If the temperature is high and close to the glass transition temperature of the underlying dry film, heating causes softening of the dry film and makes them susceptible for the solvent of the wet film above. Dissolution and poor uniformity result. On the other hand, if the heating temperature is low, the solvent is expelled too slowly and dissolution still results. Furthermore, the dissolution in this case does not only cause a vertical gradient of the composition as the case of blade-spin but also a horizontal phase separation of the material of the first and second layers. Without the centrifugal force, the system tends to reach its thermal equilibrium state which is not a sharp and uniform bi-layer structure with a large surface energy but a random distribution of aggregates of each of the two materials with horizontal phase separation. To solve the dilemma of bottom heating, rapid drying is supplemented by top heating. Hot wind with low flowing speed and high uniformity, ensured by a wind mask, is applied from the top to accelerate wet film drying without softening the underlying dry film. As in the case of blade-spin, in blade-only, the solvent is expelled in a few seconds by the simultaneous effects of bottom heating by hot plate and top heating by hot wind. The drying occurs so quickly that there is no time for the solutes to move horizontally and form aggregates. The success of this blade-only method is based on an intricate balance among solvent evaporation, dissolution, and phase separation. In the presence of large amount of solvent, the materials are free to move and tend to reach a homogeneous equilibrium state; by the substrate and wind heating, the materials are frozen into a desired highly non-equilibrium bi-layer state. With this new drying approach, large-area multi-layer organic films can, therefore, be fabricated by blade-only method in a continuous fashion at potentially very high throughput.

The success of multi-layer deposition by blade-only method is checked by several ways, including the thickness distribution with patterned first layer, the edge sharpness of the pattern boundary, scanning-electron microscopy (SEM), as well as the absence of the first layer emission in electroluminescence. Organic film deposition is made for over 10 cm. Efficient phosphorescent and fluorescent multi-layer OLEDs are made by blade-only method. Both polymers and small molecules can be deposited as long as there is a marginal solubility. Devices up to several centimeters are demonstrated to have uniform luminance and similar efficiency as the small-area ones. In addition to OLED, blade-only method is also applied to organic solar cell. Efficiency close to spin-coating and good uniformity at large area are demonstrated. Blade-only coating method, therefore, proves to meet all conditions of multi-layer, low material waste, and continuous process for the wide-spread application of OLED as a new light source in our daily life.

II. BLADE-SPIN METHOD

In blade-spin method, the substrate is mounted on the stage of a spinner. The solution is generally deposited at the front of the blade by a pipette as shown in Fig. 1. A wet film is formed by moving the blade by hand at a speed of roughly 10 cm/s. Immediately after the blade covers the entire active region of the OLED, the spinners start to rotate until the wet film becomes dry. Certain amount of the solution is spun away from the substrate, but the fraction is much smaller than the case of spin coating. The dry film thickness is determined by the solid content in the solution, the blade gap, as well as the spin speed. As discussed above, the strong effective circular horizontal wind over the substrate quickly takes the solvent away and the film dries in a few seconds during spinning. The rapid drying prevents most of the mutual dissolution. However, some level of mixing is always present but does not seem to affect the device performance much.[11–15] In most of the results below, the cross section of the blade is a circle as shown in Fig. 2(a) with four gaps of

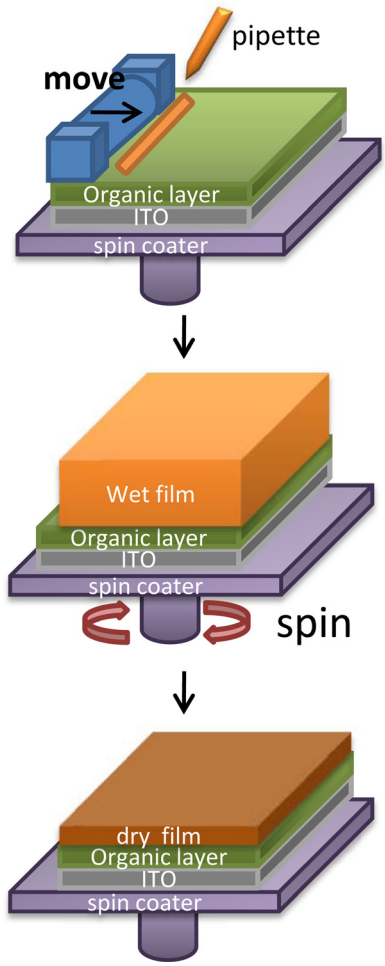

FIG. 1. (Color online) The procedure of the blade-spin method. The solution is deposited by pipette and formed a wet film by the blade coater. The thickness of the wet film is determined by the gap of the blade coater.

30, 60, 90, and 120 μm. Blade with cross section of a half circle as shown in Fig. 2(b) can also be used with similar results. The blade-only method has been applied to both polymers[10] and small molecules.[11] For blue small molecule OLED, the performance of the device made by blade-only is about 70% of the one by vacuum deposition for exactly the same material combination and structures.[11] The difference may result from the presence of some layer mixing and microscopic crystallites in the electron transport layer.[13] The major setback of blade-spin method is that the spinning step interrupts the potentially continuous blade coating process. The spinning also limits the size of the substrate to around 10 cm beyond which the sample is too heavy to be securely mounted on the spinner during rotation. If the spin step could be removed, the blade coating process could be done continuously on substrate with arbitrarily long length and in a roll-to-roll fashion if the substrate is flexible. Indeed the production throughput is expected to increase by an order of magnitude if spinning becomes unnecessary.

III. BLADE-ONLY METHOD

In blade-only method, the substrate is mounted on a hot plate in the nitrogen glove box instead of on a spinner. Immediately after the deposition of the wet film by blade coating, a gentle uniform hot wind is applied to dry the wet film in a few seconds as shown in Fig. 3. The simultaneous heating from the bottom by the hot plate and from above by the hot wind is the key to prevent mutual dissolution and ensure spatial uniformity. The total amount of solution delivered in front of the blade needs to be large enough to cover the active region yet minimized to avoid dissolution. Therefore, the solution is usually deposited as a few drops by the micropipette somewhere between the active region and the blade first. When the blade moves to the drops, the liquid spreads along the blade and fill the gap due to the capillary force. The blade then moves further through the active region and leaves a wet film behind. If there is too much solution, there

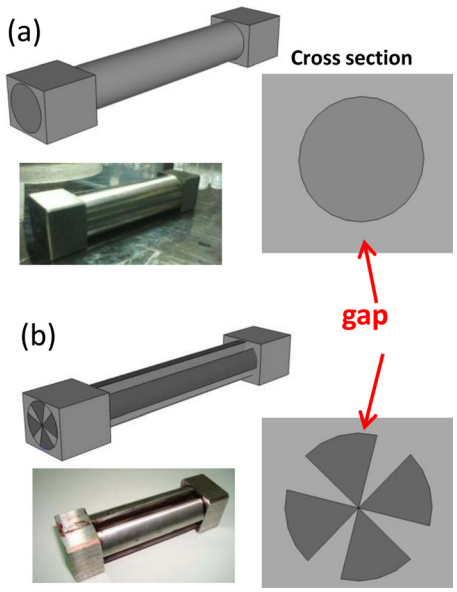

FIG. 2. (Color online) The schemes and images of (a) the circle-shaped and (b) the half circle-shaped blade coaters.

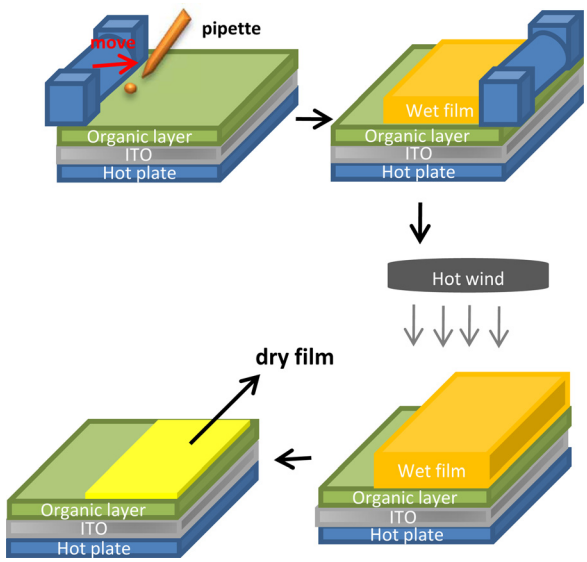

FIG. 3. (Color online) The procedure of the blade-only method. The volume of the solution is controlled precisely by macropipette. The thickness of the wet film is determined by the gap of blade coater. The hot wind is delivered from a hair dryer with wind mask.

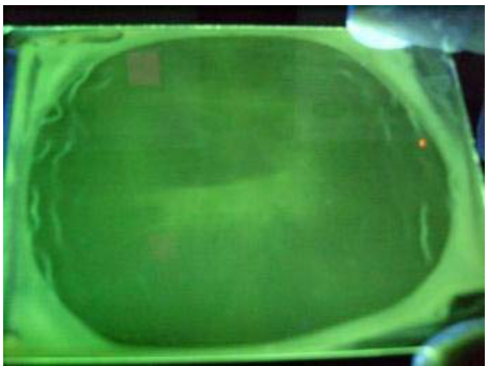

FIG. 4. (Color online) The image of the organic layers. The first organic layer is dissolved and the square is disappeared when much solution is used to form the second organic layer.

will be a pile-up in front of the blade during coating, causing dissolution as shown in Fig. 4. For most of the material and solvent combinations, the underlying dry film can withstand the solvent of the wet film of tens of microns for a few seconds. The purpose of the hot plate is to expel the solvent as quickly as possible by heating. The hot plate temperature, however, cannot be raised indefinitely. In fact for temperature over 120 °C, the first dry layer becomes soft and dissolution increases with temperature rather than decreases as wished. For temperature below the softening point, the drying of the wet film takes too much time and dissolution occurs before the solvent is expelled. Since the bottom temperature cannot be raised further, some form of heating from the top is necessary to reduce the drying time. Infrared and hot wind are possibilities of top heating. However, the apparatus for a powerful and uniform infrared source appears to be more complicated than a hot wind which proves to be very efficient to dry the wet film in seconds via a quite simple design shown in Fig. 5(a). Hair dryer supplies heated air flow with temperature up to 80 °C. The wind may cause wave in the wet film and consequently non-uniformity in the dried film if it is too strong. A wind mask shown in Fig. 5(b) is used to retard the wind and transform it from a directed air flow to a weak and uniform one. Such gently hot wind with temperature about 70 °C turns out to be very efficient and an easy way to remove all the solvent before dissolution happens and leave a uniform dry film with large area. Even though it is a heat source for not only the solvent but also the entire sample including the first dry layer, a significant temperature gradient can be maintained such that solvent is evaporated rapidly while the substrate temperature is cool enough to avoid first layer softening. Similar to bottom hot plate temperature, the temperature of the hot wind from top cannot be raised indefinitely as it may eventually heat up the first dry layer to the extend that it becomes softened and easily dissolved. The success of multi-layer blade coating without spinning, therefore, depends on an intricate balance between the bottom heating by hot plate and top heating by hot wind. Either of them alone cannot give uniform bi-layer structures.

FIG. 5. (Color online) (a) The image of the hair dryer. (b) The image of wind mask.

A. Mist and aggregate with dissolution

Below we discuss what happens when the coating parameters are not properly tuned. Non-uniformity and phase separation could result in three different scales. In the centimeter scale, uniformity problem can result if the hot wind is too strong or the bottom temperature is too low as shown in Fig. 6. Gentle and uniform hot wind through the wind mask and heating over 70 °C generally eliminates this problem. Poor

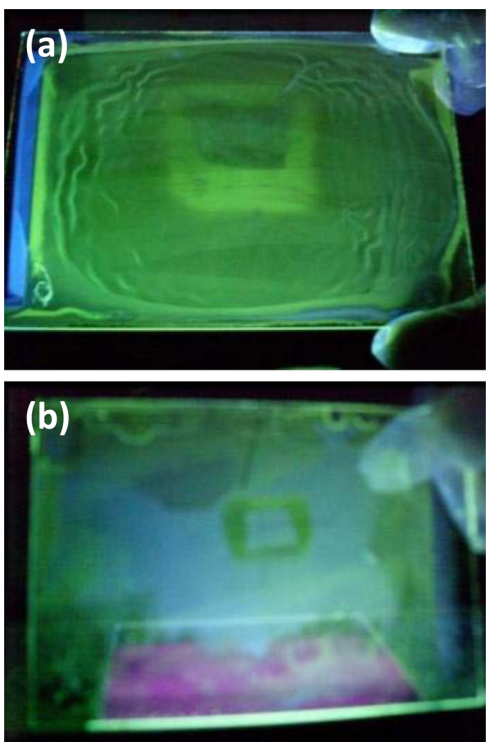

FIG. 6. (Color online) The image of the organic film made by blade-only with (a) strong hot wind or (b) low bottom heating temperature.

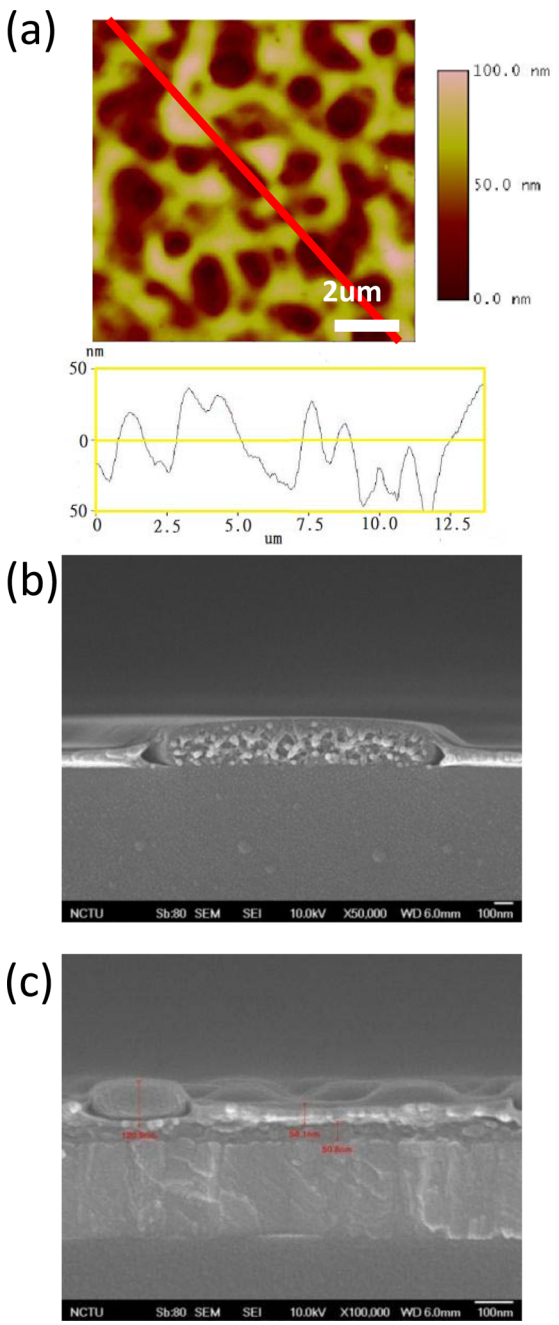

FIG. 7. (Color online) (a) The AFM image, the height profile and (b) the SEM image of TFB/PVK bi-layer structure. The PVK is dissolved in chlorobenzene. (c) The SEM image of TFB/PVK structure. The PVK is dissolved in toluene.

uniformity in the 10 μm scale can result if serious dissolution happens when the solvent is too strong for a particular first layer, usually a hole transport layer. For example, the hole transport polymer poly[(9,9-dioctylfluorenyl-2,7-diyl)-co-(4,4′-(N-(4-sec-butylphenyl))diphenylamine)] (TFB, shown in Fig. 9) has a very high solubility in chlorobenzene and roughness in the 10 μm scales result when the second layer is deposited in chlorobenzene solution even with the hot wind. Such roughness can be easily seen by naked eyes as a mist and is termed so below. The height profile of the mist is shown in Fig. 7(a), and SEM image is shown in Fig. 7(b) for TFB hole transport layer and poly(vinylcarbazole) (PVK) host as the second layer. When the solvent is changed from chlorobenzene to the weaker toluene, the mist disappears for the same material combination. However, phase separation in the 100 nm scales persist even if the film looks uniform and clear from naked eyes. The SEM image for the nano-scale phase separation, termed as aggregates below, is shown in Fig. 7(c). Even with the weak solvent of toluene and the help of the hot wind from the top, TFB apparently is still dissolved during the few seconds of emissive layer deposition with PVK host. We attribute this to the coincidence of two conditions, which are the high solubility of TFB and high surface energy for sold interface between TFB and PVK. When TFB becomes soft in the final stage of PVK wet film drying, what happens is not a slight mixing and smooth vertical composition gradient. Instead the two materials phase separate horizontally to reduce the interface area. Such aggregate formation is close to the thermal equilibrium state for the given two materials. In blade-spin method, no such aggregate forms because the centrifugal force ensures the horizontal uniformity. In fact, TFB and PVK appear to be the only studied material combination for which the blade-only method does not work even with the hot wind. Aggregates are eventually avoided by depositing only an ultrathin layer of TFB less than 15 nm thick, which is discussed below.

B. Uniform interface without dissolution

When the highly soluble TFB polymer is replaced by the less soluble hole-transport small molecule N,N′-bis (naphthalen-1-yl)-N,N′-bis(phenyl)-9,9-dimethyl-fluorene (DMFL-NPB), bi-layer coating by blade-only method can be easily achieved by high reproducibility. There is neither mist seen by the naked eyes nor aggregate in the SEM images. The hole transport material DMFL-NPB is dissolved in toluene at 1.5 wt. %. As the first layer for convenience, it is deposited by the blade-spin method with 60 μm meter gap and followed by 4000 rpm spin on the poly-(3,4-ethylenedioxythiophene)doped with poly-(styrenesulfonate) (PEDOT:PSS) anode over ITO glass. DMFL-NPB can also be deposited by blade-only method. The resulting film is 30 nm after vacuum annealing at 120 °C for 10 min. The second layer is the emissive layer of PVK:2-(4-biphenyl)-5-(4-tert-butylphenyl)-1,3,4-oxadiazole (PBD):N,N′-bis(3-methylphenyl)-N,N′-bis(phenyl)-benzidine (TPD):tris[2-(p-tolyl)pyridine]iridium(III) ($Ir(mppy)_3$) blend with weight ratio of 61:24:9:6 dissolved in toluene. Blade-only method is used to deposit the emissive layer on the dry DMFL-NPB first layer. The blend with PVK host in toluene solution of 30 μl is delivered by a pipette. The blade with gap of 60 μm moves slowly before entering the active region in order to allow an uniform spreading of the solution along the blade. Across the active region, the blade is moved by hand at a speed of roughly 40 cm/s. After blade-only coating on hot plate, the hot wind follows to rapidly expel the solvent in order to prevent dissolution of DMFL-NPB. In addition, the hot wind inhibits reflow due to short drying time which is important for large-area uniformity. The coated film is annealed in vacuum at 80 °C for 60 min, resulting in the emissive layer thickness of 60 nm. The electron transport material

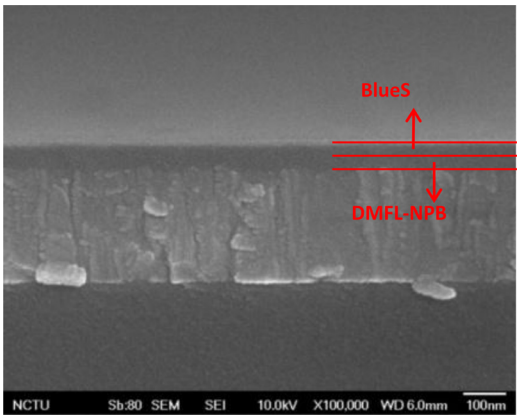

FIG. 8. (Color online) The SEM images of the bi-layer structure.

2,2′,2″-(1,3,5-benzinetriyl)-tris(1-phenyl-1-H-benzimidazole) (TPBI) can also be deposited on the emissive layer of PVK blend. TPBI is dissolved in methanol at 0.5 wt. % and 30 μl solution is delivered by a pipette. After drying in vacuum without heating, the resulting film has thickness of 25 nm.

DMFL-NPB is also successfully combined with the fluorescent emissive layer small-molecule host 1-(7-(9,9′-bianthracen-10-yl)-9,9-dioctyl-9H-fluoren-2-yl)pyrene (Blue S, shown in Fig. 9). Excellent bi-layer structure without the mist and the aggregate is made. SEM image for the bi-layer structure with Blue S host is shown in Fig. 8. The hole transport layer of DMFL-NPB is deposited in the same condition as above. The fluorescent host Blue S and blue emitter 4,4′-(1E,1′E)-2,2′-(naphthalene-2,6-diyl)bis(ethene-2,1-diyl)bis(N,N-bis(4-hexylphenyl)aniline) (Blue D) shown in Fig. 9 are mixed at weight ratio 100:2.36 in toluene at 1.5 wt. %. Blade-only method is used to deposit the emissive layer on the dry DMFL-NPB first layer on hot plate followed by hot wind as above case of the PVK blend. The coated film is annealed in vacuum at 120 °C for 10 min, resulting in the emissive layer thickness of 60 nm.

The example of DMFL-NPB and Blue S demonstrates a crucial point that the blade-only method can be applied not only to polymers like PVK but also to small molecules which are conventionally designated for vacuum deposition. Indeed due to the lack of strong interaction among the molecules and lack of chain entanglement as the case polymers, the small molecules in general do not form uniform film by spin coating in contrast to polymers. The rapid drying without spin in blade-only method exempts the small molecules from the requirement to sustain the strong centrifugal force to pull them apart. Within the few seconds of drying, the solid content of organic semiconductor molecules in the solution basically stay where they are and have no chance to reflow and result in non-uniformity, regardless whether it is polymers with strong entanglement or small molecules without entanglement.

In the molecular design for the Blue S host and DMFL-NPB hole transport material solubility is taken into consideration and so the alkyl side chains are added. The interesting next question is whether small molecules designed for vacuum evaporation, usually has no side chains and has poor solubility, form uniform films by blade coating. If the answer

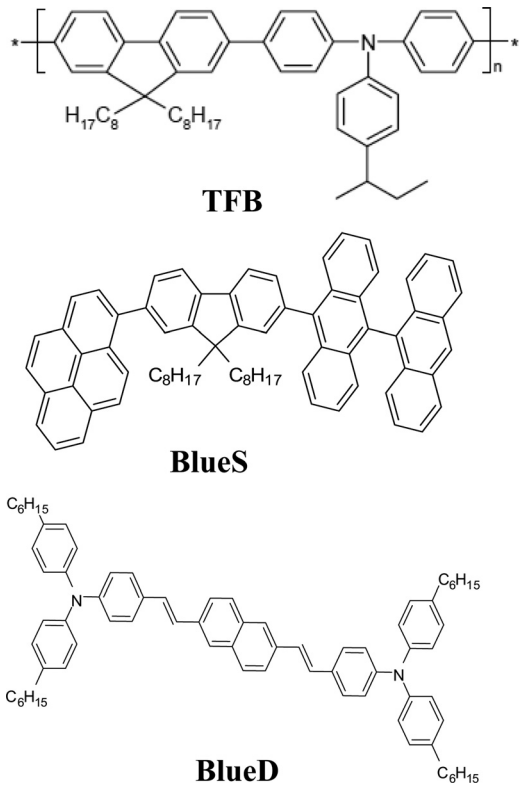

FIG. 9. The molecular structures of TFB, Blue S, and Blue D.

is yes, the exact optimal multi-layer device structures for high-efficiency small-molecule OLED by vacuum deposition can be fabricated by solution process without the need modifying the molecules, which usually result in compromised performance. The successful examples of 4,4′,4″-tris(carbazol-9-yl)triphenylamine (TCTA) and N,N′-bis(naphthalen-1-yl)-N,N′-bis(phenyl)-benzidine (NPB) are shown in Fig. 10 for hole transport layer together with 4,4′-bis(carbazol-9-yl)biphenyl (CBP) for the emissive layer host show that the answer is yes. In addition, the electron transport molecules TPBI and 3-(4-biphenyl)-4-phenyl-5-tert-butylphenyl-1,2,4-triazole (TAZ), blade-coated in our devices, are also small molecules originally designed for evaporation. The device results below show that the performance for CBP host by blade coating is about the same as the one made by vacuum deposition for exactly the same material combination and structures. The trend is, therefore, a gradual shift from polymers to modified small molecules to unmodified small molecules. The results or some key material combinations are summarized in Table I. Blade-only method does not work for polymer TFB with measurable thickness regardless of the solvent. It works well on the small molecules DMFL-NPB and TCTA even with strong solvent of chloroform.

C. Evidences of bi-layer structures

The absence of dissolution of the first layer can be confirmed by deliberately removing certain pattern in the first layer, usually a square as shown in Fig. 11(a), before the blade-only coating for the second layer. The squared is removed by a cotton stick with acetone. If the material of the first layer was dissolved by the solvent of the second layer,

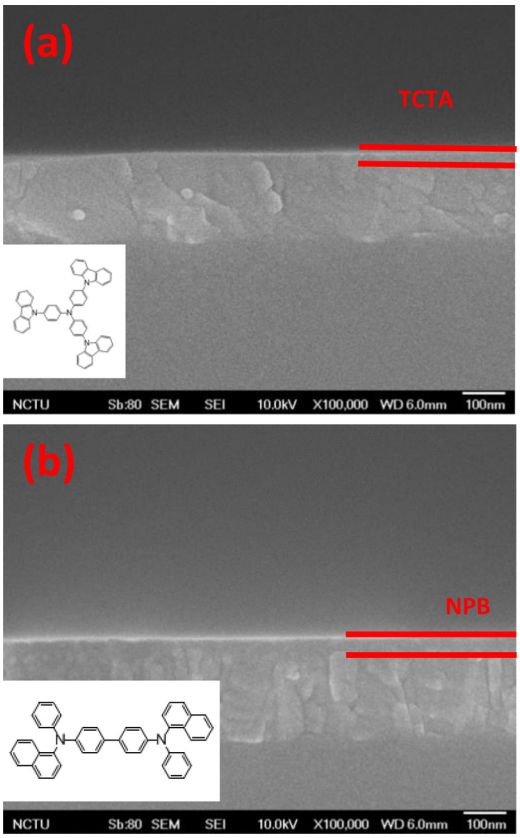

FIG. 10. (Color online) The SEM images of the (a) TCTA layer and (b) the NPB layer made by blade-only method.

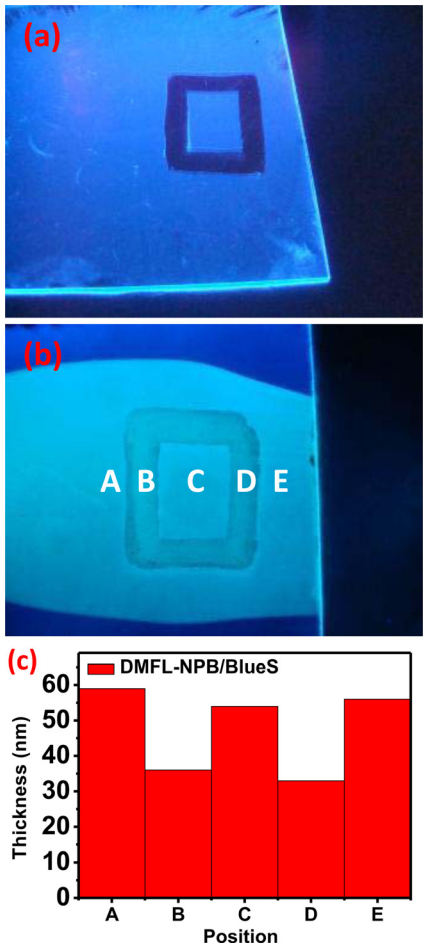

FIG. 11. (Color online) (a) The PL image of the DMFL-NPB layer with a square removed by a cotton stick with acetone. (b) The PL image of the DMFL-NPB/Blue S bi-layer. There is no detectable blur on the square edge. (c) The thickness distribution for various regions indicated in (b).

the square pattern would disappear after the coating. In Fig. 11(b), the PL image of the bi-layer film is shown for the key example of DMFL-NPB and Blue S. The square is clearly seen as the hot wind is used. On the other hand, the square is almost completely washed out if hot wind is not used. Furthermore, the sharpness of the edge of the pattern can be used to detect small level of dissolution. Assuming that the top one-third of the first layer is dissolved while the lower two-third remain intact, the edge of the square will be blurred while the square itself will still exist. Eye inspection shows that there is no detectable blur on the square edge for DMFL-NPB and Blue S, indicating that even if there is certain amount dissolution and mixing at the interface, it is small and negligible. On the other hand, if the coating parameters are not properly tuned, one will see the significant distortion or disappearance of the square pattern.

The total film thickness of the bi-layer structure with a square in the first layer also needs to be checked to confirm the success of blade-only coating. Outside the square, there is a bi-layer structure so the total thickness, measured by surface roughness meter Kosaka ET4000, should be the sum of the thicknesses of the first and the second layers. On the other hand, inside the square, there is no first layer so the thickness should be the same as the expected second layer. Fig. 11(c) shows the thickness distribution for the region containing the square for the example of DMFL-NPB and Blue S. Indeed the difference between the region outside and inside the square is what one expects for the thickness of the second layer. For other important material combinations, the thickness distributions are shown in Figs. 12(b) and 12(d). Combining the correct thickness distribution and the sharp edge of the square pattern after coating, we conclude that blade-only method can be used to deposit the second layer on top of the first layer for a wide range of materials.

TABLE I. The results of various HTL and EML combination.

HTL	EML host	Solvent	Wind	Mist	Aggregate
TFB	PVK	Chlorobenzene	Y	Y	Y
TFB	PVK	Toluene	Y	N	Y
DMFL-NPB	PVK	Toluene	Y	N	N
DMFL-NPB	Blue S	Toluene	Y	N	N
TCTA	CBP	Chloroform	Y	N	N

The PL images and the thickness distribution with a square for other hole transport layer (HTL)/emissive layer (EML) examples are shown in Fig. 12. The results with and without the hot wind followed by blade coating are compared. The hot plate is fixed at 80 °C for all cases. In general, the hot wind significantly reduces dissolution and improves the uniformity. For the cases of DMFL-NPB/PVK, TFB/poly(9,9-dioctylfluorene), and TCTA/CBP, the square pattern is visible even without the hot wind, suggesting less

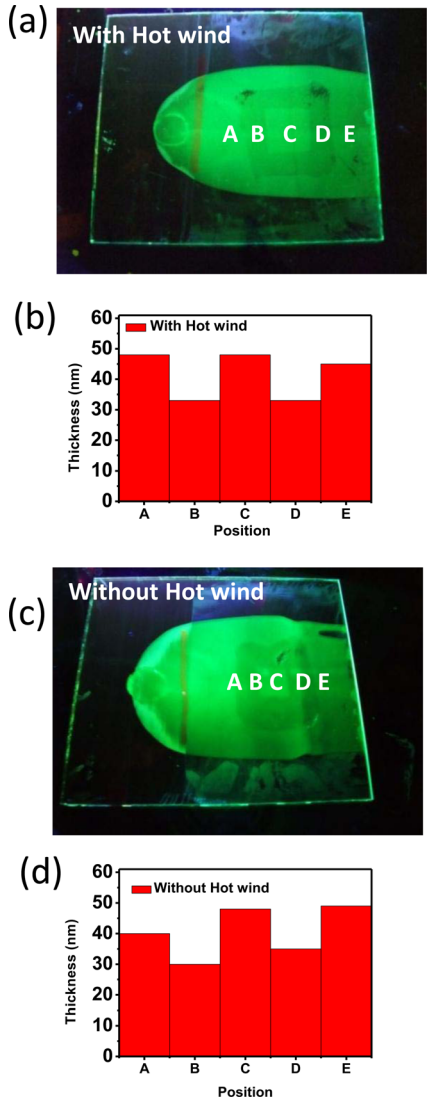

FIG. 12. (Color online) The PL images of the TCTA/CBP layers made by blade-only (a) with and (c) without hot wind. The thickness distribution of the TCTA/CBP layers (b) with and (d) without hot wind.

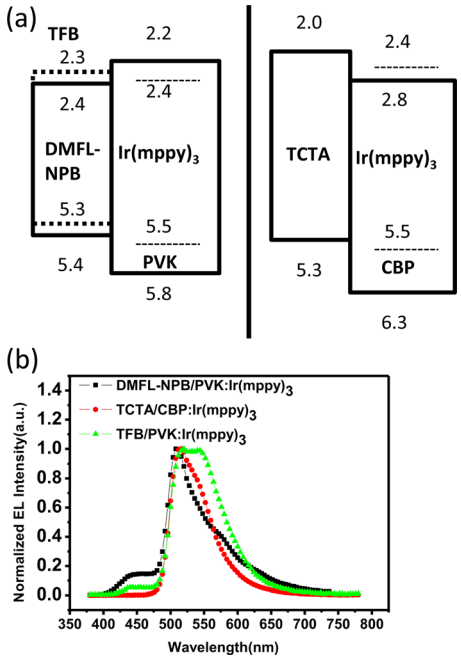

FIG. 13. (Color online) (a) The HOMO and LUMO levels of various HTL and EML layers. The EL spectrum of (b) the DMFL-NPB/PVK:Ir(mppy)$_3$ bi-layer, the TCTA/CBP: Ir(mppy)$_3$ bi-layer, and the TFB/PVK: Ir(mppy)$_3$ bi-layer. The stronger blue emission is observed in DMFL-NPB/PVK:Ir(mppy)$_3$ and TFB/PVK:Ir(mppy)$_3$ case.

tendency for the emissive material and hole transport layer to mix. The edge of TCTA/CBP is, however, blurred without the hot wind. The uniformity is unacceptable without the hot wind. For another case of PVK/TPBI, no matter TPBI was dissolved in methanol or toluene, the square pattern is clear as long as the hot plate and hot wind are used.

Electroluminescence spectrum provides yet another strong evidence of the absence of dissolution. In case of dissolution, the hole transport layer and the emissive layer are mixed together to be a blend. The hole transport molecules are, therefore, in contact with the electron transport layer. Most of the hole transport molecules have a blue fluorescence themselves. In the case of mixing, the electrons can be injected from the electron transport layer into the lowest unoccupied molecular orbital (LUMO) level of the hole transport material and recombine with the holes in their HOMO level to emit light. On the other hand, in the bi-layer structure, the electrons are transported in the LUMO level of the emitter and the hole transport layer does not have a contact with the electron transport layer. There is usually a much larger electron injection barrier from the emitter LUMO level to the hole transport layer LUMO layer because of the low-lying emitter LUMO level as shown in Fig. 13(a). Consequently, in the multi-layer structure due to the electron blocking at the HTL/EML interface, there is electron and thus no recombination in the hole transport layer. The absence of the blue emission from the hole transport layer is, therefore, an evidence of no mixing. The electroluminescence spectra for the combination of DMFL-NPB/PVK, and TCTA/CBP for HTL and EML are shown in Fig. 13(b). The emission peak for DMFL-NPB is at 458 nm, while TCTA is at 385 nm. The spectrum only comes from the emitter and there is completely no HTL emission, indicating the success of multi-layer structure with efficient electron blocking in TCTA/CBP case. For comparison, the failed example of TFB/PVK gives strong blue emission from TFB in Fig. 13(b), consistent with the horizontal phase separation and aggregate formation shown in Fig. 7(c) above. Another failed example is DMFL-NPB/PVK because of the lower LUMO of DMFL-NPB.

D. Large-area uniformity

One of the great advantages of blade-only method is its ease to scale up to large size. In the blade-spin method, the spinning itself limit the substrate size and weight. In blade-only coating, in principle, there is a translational invariance along the blade direction except for the region near the blade edge. In practice, the uniformity along the blade direction is affected by the factors below. First, the glass substrate needs to have a height variation no more than 1/10 of the blade gap, corresponding to glass evenness within 10 μm. Such requirement is met by the glass from commercial sources.

We measured that the glass evenness is about 8 μm cross a region of 10 cm. Second, the top heating should be uniform. This is why a wind mask shown in Fig. 5 is required to produce a gentle and uniform hot wind. Third, the solution piled up in front of the blade gap cannot have a large variation in its amount as the wet film thickness left behind by the blade motion depends on the amount of solution in the front. A multiple-head micropipette can be used to deliver a series of liquid drops in front of the blade. Assisted by the capillary force, the liquid spread uniformly along the blade head before the blade enters the active region as shown in Fig. 14. When the three factors are properly taken into account, good uniformity along the blade direction can be realized for blade as large as 20 cm. The uniformity along the motion direction, i.e., perpendicular to the blade direction, is another issue. First, the blade motion needs to have a stable speed. In this work, the blade is moved by hand. For instances that the hand motion happens to be not smooth, uneven film thickness along the motion direction results, apparently because the wet film thickness decreases with the blade motion speed. The motion speed stability issue can be solved by a mechanic motion controlled by a motor. Multiple-head micropipette is used to deposit three drops of solution in front of the initial position of the blade as shown in Fig. 14. The blade moves first slowly to cover the liquid drops such that an even liquid distribution is reached before the blade enters the active region as shown in Fig. 14. Once near the active region, the blade move steadily at rough speed of 40 cm/s. The whole process is done by hand inside a nitrogen glove box with the same conditions as the small area cases discussed above. The second factor of the uniformity along motion direction is the amount of solution left in front of the blade gap. As the solution is running out, the wet film becomes thinner and thinner. A large amount of initial solution deposition could, in principle, prevent the solution from running out for a long distance. Unfortunately such large amount of solution will cause dissolution of the first layer because of the increase in the piled-up amount in front of the blade during motion. In fact, the solution delivery needs to be minimized to avoid dissolution. In practice, for 15 μl per drop and 5 mm between the drops in the initial delivery in front of the blade, there is no dissolution altogether and uniformity along the motion direction can be kept up to about 5 cm. The one-dimensional overall thickness distribution for large area is shown in Fig. 15. The variance is within 10 nm for an average of 80 nm, enough to produce uniform electroluminescence to be discussed below. The limit on the uniformity along the motion direction can be lifted if the solution delivery is changed from the current single shot delivery to a continuous delivery. Such continuous delivery is also necessary for the future roll-to-roll process of blade-only method for arbitrarily large substrate.

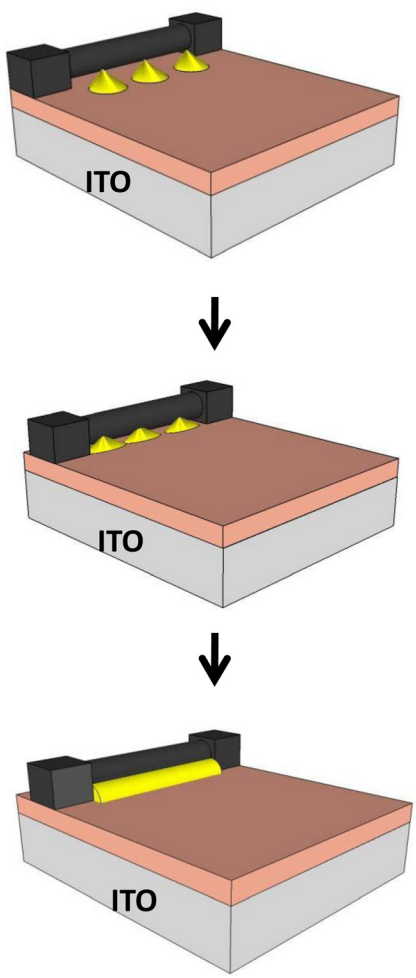

FIG. 14. (Color online) The procedure of the blade-only method.

E. PEDOT:PSS by blade-only method

In addition to the organic semiconductors, the conducting polymer PEDOT:PSS used as the OLED anode on top of ITO can also be deposited by blade-only method. PEDOT:PSS (CLEVIOS™ P VP AI4083) in water solution from 1.3 wt. % to 1.7 wt. % is further diluted by water with 1:1 weight ratio before blade coating. Without dilution the thickness will be too large. Two 50 μl drops of diluted PEDOT:PSS solution is deposited on ITO glass by a pipette. The hot plate temperature is 90 °C and the hot wind condition is the same as above. After coating, the film is annealed at 200 °C for 15 min. The resulting dry film has the optimal thickness of 45 nm. Even though there is no concern of dissolution for PEDOT:PSS coating, both the hot plate and the hot wind are still necessary for uniformity. Without them,

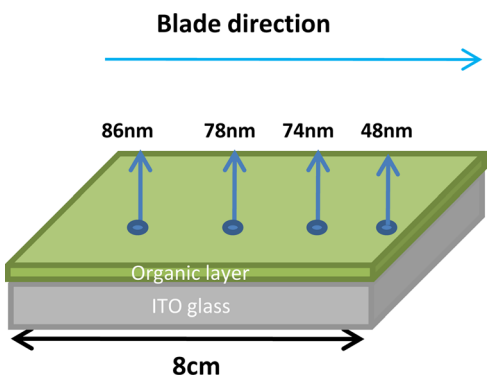

FIG. 15. (Color online) The thickness distribution of the PVK:PBD:TPD:Ir(mppy)$_3$ layer.

spots with high thickness form as shown in Fig. 16(a). Without the hot wind but with the hot plate, there is a decrease of thickness from 85 nm to 50 nm along the blade motion direction. When both the hot plate and the hot wind are used for mean thickness of 45 nm, the thickness variation of PEDOT:PSS is less than 10 nm for a range of 5 cm. Apparently, the inhibition of reflow is crucial to deposit even a single layer by blade-only coating. The OLED device performance is the same for spin-coated and blade-coated PEDOT:PSS as discussed below.

IV. DEVICE CHARACTERISTICS

Below we present the device characteristics for small area of 2 mm by 2 mm first. Large area devices will be discussed later. We first cover phosphorescent then fluorescent devices. The PEDOT:PSS layer is deposited by either standard spin coating or blade-only coating. The ultrathin hole-transport polymer TFB is deposited by either spin-rinse method or blade-only method. Such ultrathin TFB gives higher efficiency than a cross-linked hole transport layer with more typical thickness of tens of nanometers. Various small-molecule electron transport layers are compared.

For standard spin coating, PEDOT:PSS (CLEVIOS P VP AI 4083) in water solution is spin coated at 2000 rpm for 40 s, then annealed in air at 200 °C for 15 min, resulting in film thickness of 40 nm. For spin-rinse method of TFB, 1 wt. % of TFB in toluene solution is deposited first by blade-spin method at 2000 rpm for 30 s, then annealed in vacuum at 180 °C for 40 min. To remove the dissolved part, the TFB film is rinsed by pure toluene at 4000 rpm, resulting in an ultrathin film below 10 nm. Such thin TFB significantly improves the hole injection from the PEDOT:PSS into the PVK host due to the large hole barrier.

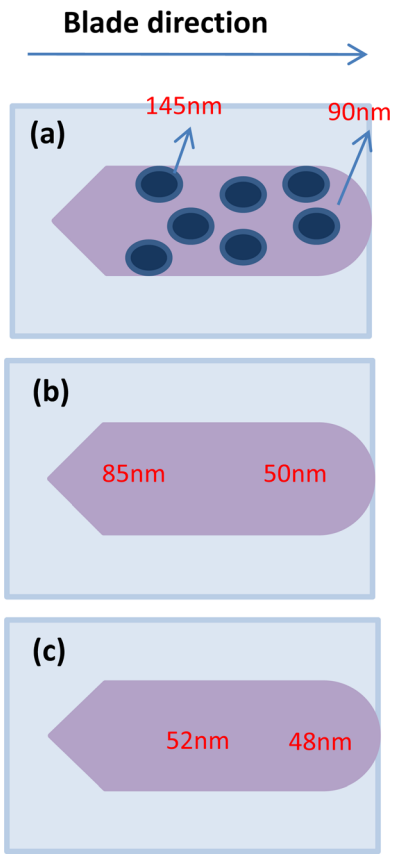

FIG. 16. (Color online) The thickness distribution of PEDOT:PSS made by blade-only (a) without hot wind and hot plate, (b) without hot wind but with hot plate, and (c) with hot wind and hot plate.

A. Green phosphorescence with PVK host

The emissive layer of PVK:PBD:TPD:Ir(mppy)$_3$ with weight ratio 61:24:9:6 is deposited by blade-only method described above. The hot wind is applied for 5 s after blade coating. The film is then annealed in vacuum at 80 °C for 60 min. The resulting thickness is 65 nm. 15 nm of TPBI is deposited by blade-only method in methanol solution as described above. Finally, LiF of 0.8 nm and Al of 100 nm are evaporated as the cathode. This cathode is used for all devices in this work except solar cell. The device is encapsulated in nitrogen glove box and measured in air by spectrophotometer PR650. The peak current efficiency for the green emission is 25 cd/A at 10 V, with peak luminance over 20 000 cd/m^2. These results are the same as the devices with spin-coated emissive layer of PVK blend,[13] indicating that blade-only method gives almost the same microscopic morphology for the quaternary blends. The uniform dispersion of the emitter Ir(mppy)$_3$ in the host is necessary to achieve such high efficiency. Apparently neither the hot plate nor the hot wind causes aggregation of the emitter and other two small molecules in PVK polymer host.

Now, we replace the spin-rinse method for the ultrathin TFB by blade-only method. Dilute solution of TFB is used to give barely enough thickness on PEDOT:PSS. Too much TFB will cause mixing of it with the second emissive layer and blue emission in device. Too little TFB is not enough to assist hole injection into PVK blend. TFB in toluene solution with concentration of 0.5 wt. %, 0.6 wt. %, and 0.7 wt. % are compared. The solution is blade coated on PEDOT:PSS with blade gap of 60 μm on hot plate of 90 °C followed by hot wind. The resulting thicknesses are 15 nm, 16 nm, and 17 nm. Such thickness is so small that the majority of the TFB sticks to the underlying PEDOT:PSS and is not dissolved in the following steps despite of the high solubility of TFB. As shown in Fig. 17 for TFB solution with 0.6 wt. %, there is an optimal device efficiency about 25 cd/A which is the same as the one by spin-rinse above. The peak luminance around 20 000 cd/m^2 is also similar. Note that for 0.7 wt. % TFB, the efficiency drops to 13 cd/A and blue TFB emission becomes visible. So far, the PEDOT:PSS layer is deposited by the standard spin coating. When it is replaced by blade-only coating described above to yield a thickness of 45 nm, the device performance for the same PVK:PBD:TPD:Ir(mppy)$_3$ blend has little difference as shown in Fig. 18. In particular, the efficiency of 28.7 cd/A is reached at 12 V. This indicates that the hot plate and hot wind do not cause phase separation problem for PEDOT and PSS components.

In addition to TPBI, some other common electron transport small molecules are deposited on the emissive layer of PVK:PBD:TPD:Ir(mppy)$_3$ by blade-only method for comparison. TAZ shown in Fig. 19 is dissolved in methanol at

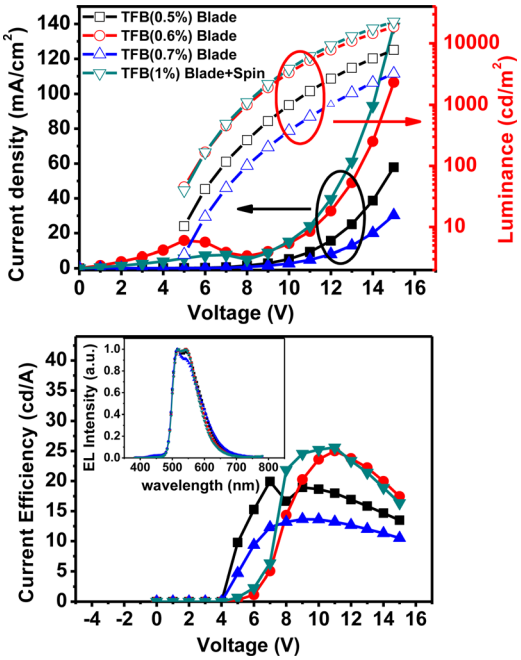

FIG. 17. (Color online) The (a) current density, the luminance, and (b) the current efficiency of the green phosphorescence devices with different thickness of the hole transport layer. The inset in (b) shows the spectrum of the devices.

1 wt. %. 30 μl drop by pipette gives 40 nm film thickness with 80 °C followed by hot wind as above. 20 μ1 of 1 wt. % solution gives 30 nm thickness. As shown in Fig. 20(c) for 40 nm TAZ, the device performance is similar to TPBI discussed above with peak efficiency of 22 cd/A. However, the current density and luminance drops significantly when TAZ thickness is reduced to 30 nm, probably due to the reduced

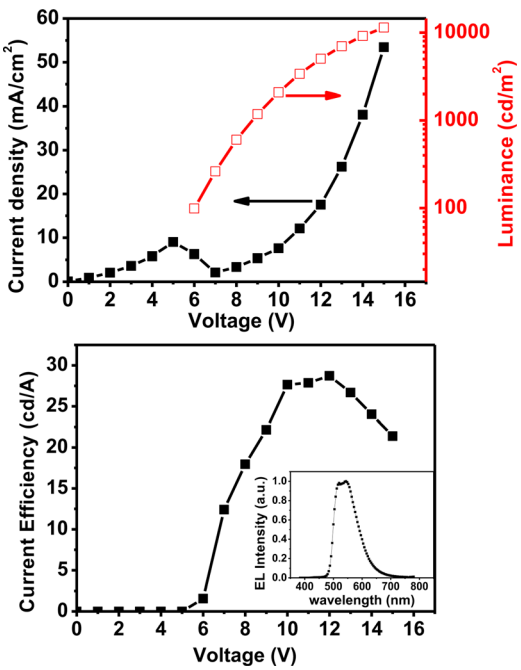

FIG. 18. (Color online) The (a) current density, the luminance and (b) the current efficiency of the green phosphorescence device. Each layer of the device is made by blade-only method. The inset in (b) shows the spectrum of the device.

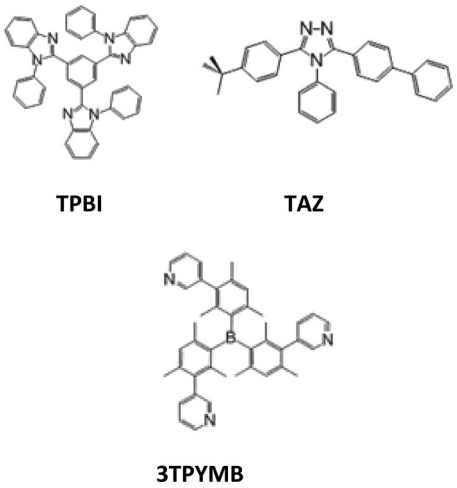

FIG. 19. The molecular structures of TPBI, TAZ, and 3TPYMB.

electron injection. Tris(2,4,6-trimethyl-3-(pyridin-3-yl)phenyl)borane (3TPYMB) shown in Fig. 19 of 30 nm can be deposited by blade-only method with 20 μl of 1 wt. % solution in chlorobenzene. The current density and luminance is, however, even lower as shown in Figs. 20(a) and 20(b). This is probably because of mixing with the emissive layer due to the strong solvent of chlorobenzene.

The ultrathin TFB is compared with a cross-linking hole transport material of DV-Me-TPD shown in Fig. 21, whose synthesis is to be published elsewhere. The cross-linking molecule is dissolved in toluene at 0.6 wt. % then deposited by blade-only method to yield film thickness of 25 nm. After annealing at 180 °C in nitrogen for 30 min, the molecules are thermally cross-linked and the film becomes insoluble. For the same process conditions of the PVK:PBD:TPD:Ir(mppy)$_3$ emissive layer and TPBI electron transport layer, the device performance is shown in Fig. 22. The efficiency drops while the luminance is similar to the TFB. There is no blue emission from the HTL suggesting that there is a good electron blocking. The electron-hole balance of the PVK blend may be nearly optimized in the particular weight ratio of the PBD and TPD for electron and hole transport, respectively. There is, therefore, no need of electron blocking layer to raise recombination. In contrary, the introduction of electron blocking layer of common thickness of 25 nm by cross-linking method appears to interrupt the carrier balance and reduce the efficiency. In fact, cross-linking appears to be completely unnecessary given the general applicability of blade-only method to a wide range of material combinations without cross-linking functional groups.

B. Orange, blue, and white phosphorescence with PVK host

Other colors can be obtained by replacing the green Ir(mppy)$_3$ by other iridium complex in the PVK blend. For orange red emission peaked at 588 nm, the iridium complex emitter tris[2-(4-n-hexyl-phenyl)quinoline]iridium(III) (Hex-Ir(phq)$_3$) shown in Fig. 23 is used. This emitter molecule has a six-carbon alkyl side chain to increase the solubility and dispersion with the host. The 61:24:9:6 weight ratio for Ir(mppy)$_3$

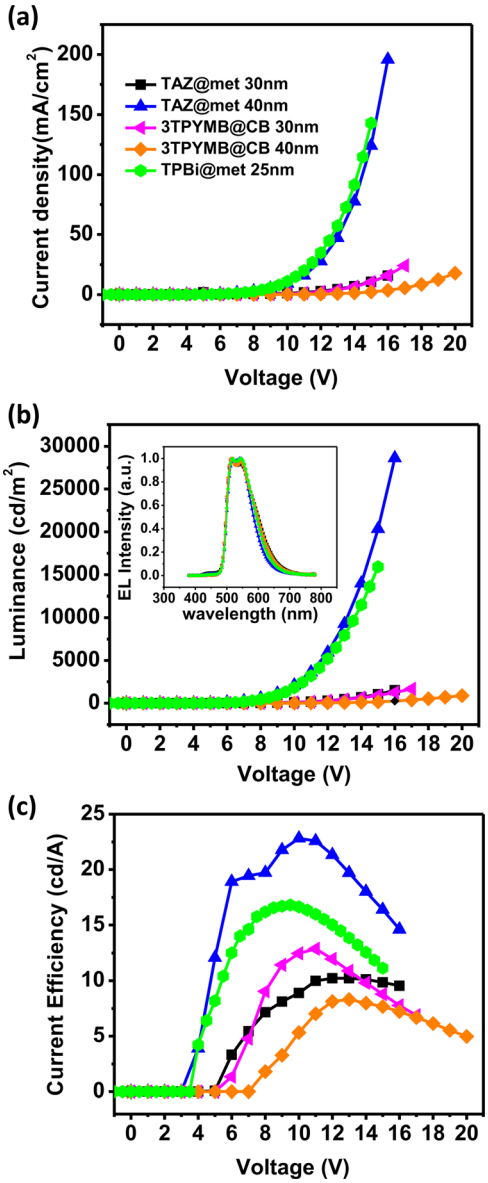

FIG. 20. (Color online) (a) The current density, (b) the luminance, and (c) the current efficiency of the devices with different electron transport layers. The inset in (b) shows the spectrum of the devices.

is kept for Hex-Ir(phq)$_3$ in the blend. PEDOT:PSS is spin-coated and TFB is spin rinsed. The blade-only coating conditions are the same as above for the emissive and electron transport TPBI. The device performance is shown in Fig. 24. Peak efficiency of 13 cd/A is reached at 6 V and peak luminance of 8000 cd/A at 11 V. This result is slightly lower than the efficiency of 17 cd/A in blade-spin device with Hex-Ir(phq)$_3$ emitter.[15] Another orange emitter iridium(III) bis(4-(4-t-butylphenyl)thieno[3,2-c]pyridinato-N,C$^{2\prime}$)acetylacetonate (PO-01-Hex) shown in Fig. 23 is used as the orange emitter with peak at 580 nm. The material ratio in the host and all process conditions are the same as Hex-Ir(phq)$_3$. The device performance is shown in Fig. 25. Peak efficiency of 15 cd/A is reached at 7 V while peak luminance of 18 000 cd/m^2 is reached at 10 V.

Blue phosphorescence can be obtained by using the emitter bis(3,5-difluoro-2-(2-pyridyl)phenyl-(2-carboxypyridyl)iridium(III) (FIrpic) shown in Fig. 23 with triplet exciton energy of 2.65 eV.[16] The triplet exciton energy of PBD and

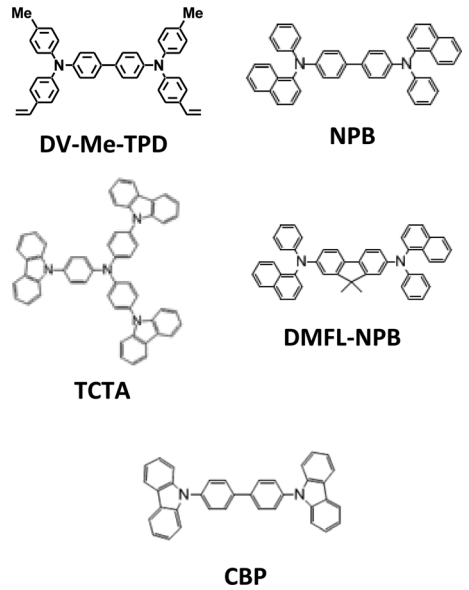

FIG. 21. The molecular structures of DV-Me-TPD, NPB, DMFL-NPB, TCTA, and CBP.

TPD, 2.46 and 2.3 eV respectively,[17,18] are too low to confine the exciton in FIrpic, so it is replaced by another electron transport molecule 1,3-bis[2-(4-tert-butylphenyl)-1,3,4-oxadiazo-5-yl]benzene (OXD-7) with triplet exciton energy of 2.7 eV.[17,18] The emissive layer is a blend of PVK:OXD-7:FIrpic with weight ratio of 69:21:10. Chlorobenzene solution of 1 wt. % is deposited by blade-only method with blade gap of 60 μm meter on hot plate of 80 °C followed by hot wind to give thickness of 75 nm. TPBI is deposited by blade-only method as above. The efficiency is 8 cd/A at 9 V and peak luminance is over 3000 cd/m^2 as shown in Fig. 26. White emission can be obtained by adding a small amount of orange

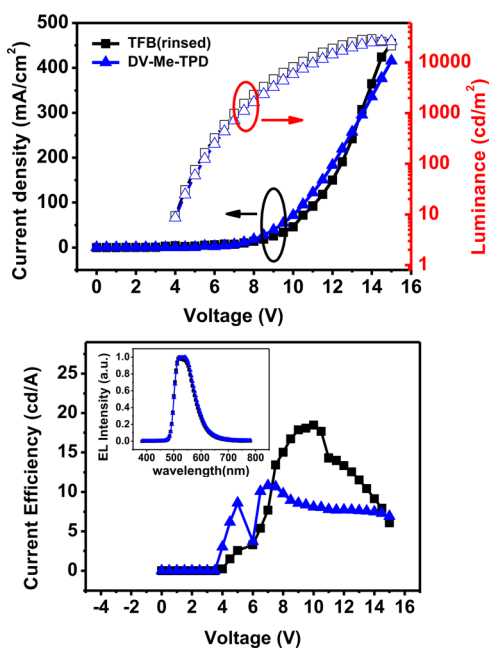

FIG. 22. (Color online) (a) The current density, the luminance, and (b) the current efficiency of the green phosphorescence devices using cross-linkable hole transporting layer. The inset in (b) shows the spectrum of the devices.

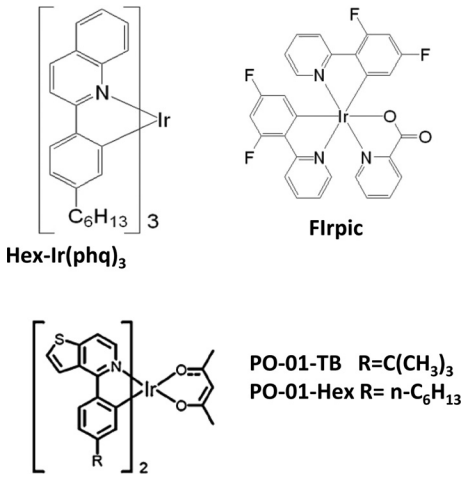

FIG. 23. The molecular structures of the Hex-Ir(phq)$_3$, the PO-01-TB, the PO-01-Hex, and the FIrpic.

emitter for the FIrpic device. Hex-Ir(phq)$_3$ is added with 1:55 ratio to FIrpic in the emissive layer. For the sample fabrication condition as the pure FIrpic device above the results are shown in Fig. 27. White emission with Commission Internationale de L'Eclairage (CIE) coordinate of (0.38, 0.39) is obtained, but the efficiency is only 6 cd/A at 12 V. Similarly, the orange emitter PO-01-Hex is mixed with FIrpic at ratio of 1:40 to yield white emission with CIE coordinate of (0.32, 0.44) shown in Fig. 28. The peak efficiency is only 9 cd/A at 12 V. The orange emitters in the blends apparently act as carrier traps so the operation voltage becomes much higher than the pure FIrpic device. PVK blend around 60 nm is, therefore, not suitable for high-efficiency white OLED due to both the low triplet level and the high impedance. Multi-layer structures with reduced emissive layer thickness and host with high triplet level are required to improve the white OLED efficiency by blade coating.

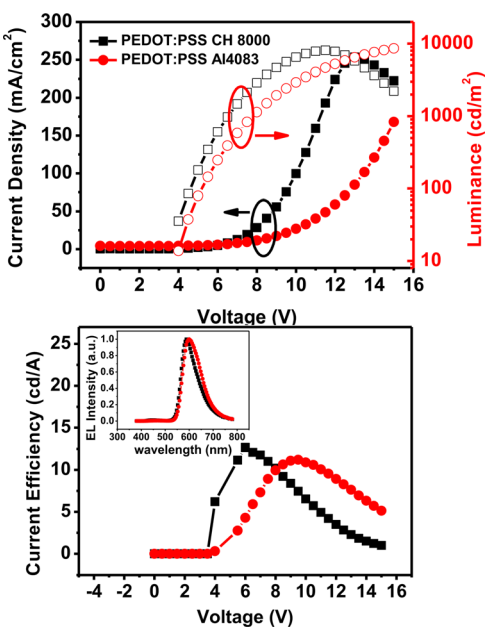

FIG. 24. (Color online) (a) The current density, the luminance, and (b) the current efficiency of the red phosphorescence devices with different types of PEDOT:PSS. The inset in (b) shows the spectrum of the devices.

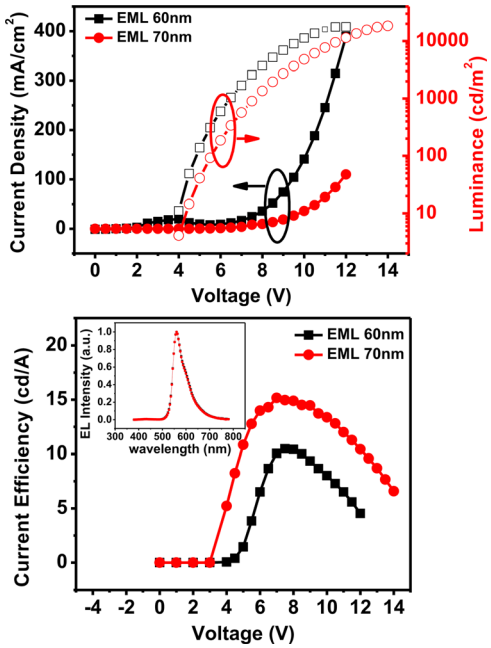

FIG. 25. (Color online) (a) The current density, the luminance, and (b) the current efficiency of the red phosphorescence devices with different thickness of the emission layers. The inset in (b) shows the spectrum of the devices.

C. Fluorescence

So far, we consider phosphorescent devices. Following we turn to discuss fluorescent devices, all with Blue S shown in Fig. 9 as the host. Various fluorescent emitters are introduced into the Blue S host to produce various colors including white. First, the blue emitter Blue D shown in Fig. 9 is mixed with Blue S with the Blue S:Blue D weight ratio of 100:2.36 as described above. The hole transport layer DMFL-NPB is deposited by blade-spin method over

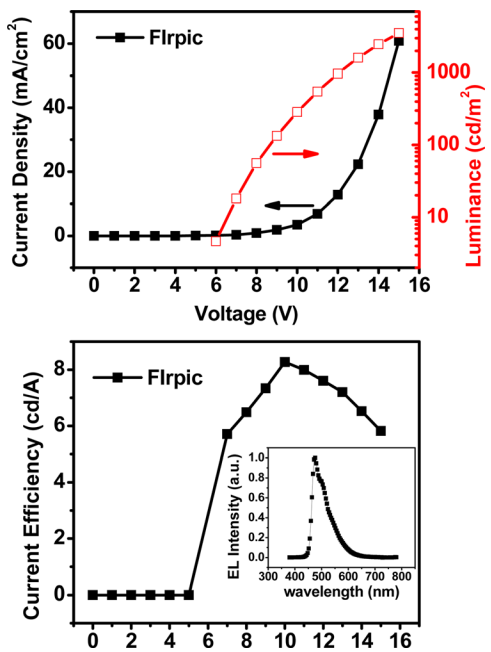

FIG. 26. (Color online) (a) The current density, the luminance, and (b) the current efficiency of the blue phosphorescence device. The inset in (b) shows the spectrum of the device.

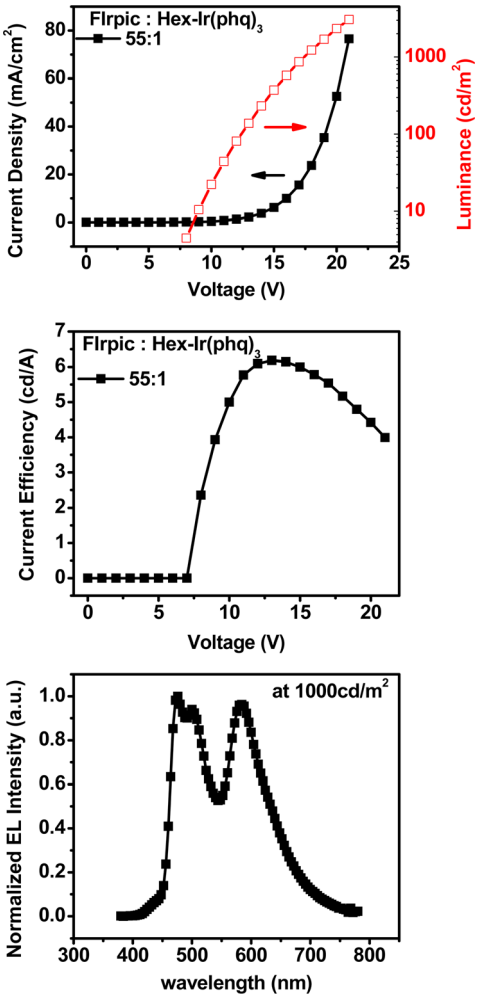

FIG. 27. (Color online) (a) The current density, the luminance, (b) the current efficiency and (c) the spectrum at 1000 cd/m^2 of the white phosphorescence device. The dopant ratio of FIrpic and Hex-Ir(phq)$_3$ is 55:1.

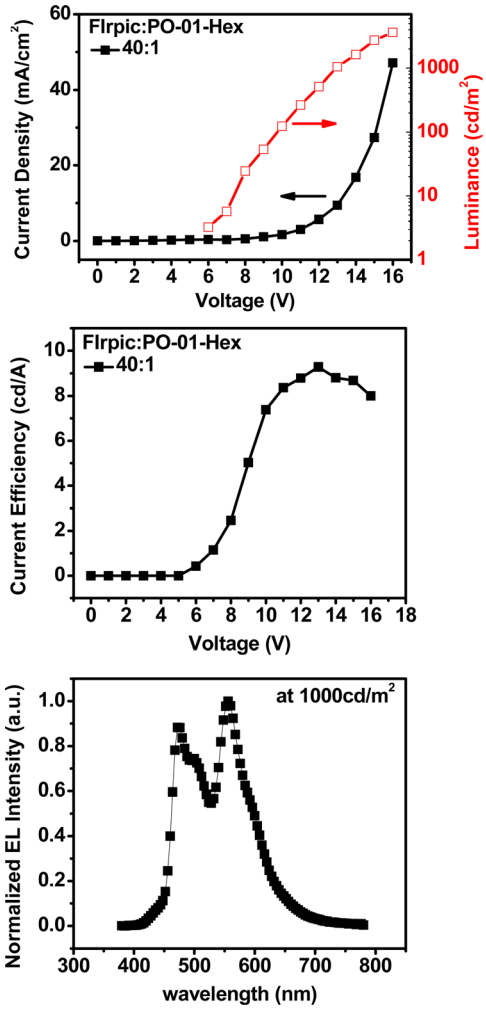

FIG. 28. (Color online) (a) The current density, the luminance, (b) the current efficiency, and (c) the spectrum at 1000 cd/m^2 of the white phosphorescence device. The dopant ratio of FIrpic and PO-01-Hex is 40:1.

PEDOT:PSS with 1.5 wt. % in toluene and 4000 rpm following blade coating. The resulting thickness is 30 nm. The Blue S:Blue D emissive layer is deposited by blade-only method described above, with 1.5 wt. % in toluene with blade gap of 60 μm meter and 20 μl of solution drop. The film is annealed at 120 °C in vacuum for 10 min, resulting in thickness of 60 nm. TPBI of 20 nm is deposited by blade-only method as above in 0.5 wt. % in methanol. LiF/Al is evaporated as the cathode. The blue device performance is shown in Fig. 29. Peak efficiency of 4.2 cd/A is reached at 6 V, with peak luminance around 20 000 cd/m^2. The efficiency is slightly lower than the 7 cd/A obtained in vacuum deposition for the same device structure. The brightness is even higher. The green emitter 2,3,6,7-tetrahydro-1,1,7,7,-tetramethyl-1H, 5H,11H-10-(2-benzothiazolyl)quinolizino[9,9a,1gh]coumarin (C545T) shown in Fig. 30 is used in Blue S host with 100:2.5 weight ratio. For the same thickness and fabrication conditions as the Blue D emitter, the green device performance is shown in Fig. 31. The peak efficiency of 5 cd/A is reached at 10 V while the peak luminance is over 25 000 cd/m^2. The result for similar device with 4-(dicyanomethylene)-2-tert-butyl-6-(1,1,7,7-tetramethyljulolidin-4-yl-vinyl)-4H-pyran (DCJTB) orange red emitter at Blue S:DCJTB weight ratio of 100:1.5 is shown in Fig. 31. Peak luminance of 9 cd/A is reached at 7 V while the peak luminance is about 20 000 cd/m^2. There is, however, some host emission probably due to the aggregation of DCJTB in the host. For the orange emitter 4-(dicyanomethylene)-2-methyl-6-julolidyl-9-enyl-4H-pyran (DCM2) with 100:1 weight ratio in Blue S, the efficiency drops to 3.0 cd/A with a stronger host emission. For 5,6,11,12-tetraphenylnaphthacene (Rubrene) as the orange emitter with 100:1 weight ratio in Blue S host, the efficiency is 7 cd/A at 8 V and the peak luminance is over 15 000 cd/m^2 as shown in Fig. 31. Finally, white emission is obtained by adding simultaneously Blue D and Rubrene emitters into the host with the Blue S:Blue D:Rubrene ratio of 100:2.36:0.236. CIE coordinate of (0.33, 0.4) is achieved with peak efficiency of 6.7 cd/A at 6 V. Peak luminance is about 25 000 cd/m^2 as shown in Fig. 32. As fluorescent devices, the DMFL-NPB/Blue S host combination has good efficiency and high luminance for all colors. They have several advantages over conventional fluorescent conjugated polymers based on PPV and PF including high material purity, absence of batch to batch variation inevitable for polymers, and finally great flexibility for the set of emitters to tune the emission color.

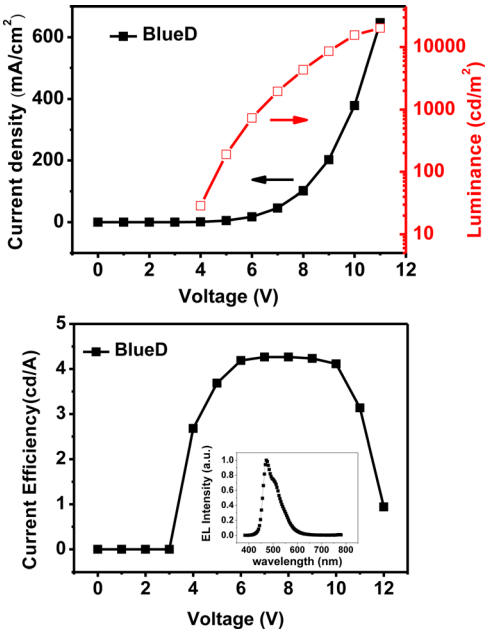

FIG. 29. (Color online) (a) The current density, the luminance, and (b) the current efficiency of the blue fluorescence device. The inset in (b) shows the spectrum of the device.

D. Device with large area

So far, the device results are for an active region of 2 mm by 2 mm. Below we present characteristics for devices with active region of 2 cm by 3 cm fabricated by blade-only method as described above in Sec. III D. Uniform electroluminescence is realized, indicating good uniformity for all the three semiconductor layers. The pictures for several large-area phosphorescent and fluorescent devices driven by a 9-V battery are shown in Fig. 33. The luminance distribution across the active region is shown in Fig. 34, where variance is less than 10%. Uniformity can be further improved if the blade motion is controlled automatically. The device characteristics for the large area devices are shown in Fig. 34. In general, the current density and luminance as functions of voltage are almost the same as the small devices.

Scaling up of the blade-coated area for the multi-layers of organic films to over 20 cm by 20 cm region is expected if the solution delivery is changed from single shot to continuous. Even for single delivery, uniform film is obtained for a region of 20 cm by 5 cm, where 20 cm is along the blade and 5 cm along the motion directions. There is, however, a limit on the OLED active region size due to the ITO sheet resistance. For large-area blade coating, the coated film will cover an array of active regions no more than about 5 cm by 5 cm for uniform luminance. Simple estimate shows that beyond that size, the ITO sheet resistance cause enough voltage drop across the active region such that luminance variation can be seen by human eyes. The voltage drop in ITO can be estimated in the picture shown in Fig. 35. Assuming the vertical current density J_B is a constant, the horizontal current density J_S in ITO must satisfy $(dJs/dx)t = J_B$, where t is the ITO thickness, because the vertical current consumes the horizontal current. Take the boundary condition for J_S at the end of the device as $J_S(L) = 0$, we get $Js(x) = J_B(x/t)$. The horizontal electric field is $E(x) = \rho Js(x)$, where ρ is the ITO resistivity. Substituting $J_S(x)$ into $E(x)$ and integrating, the voltage drop from x = 0 to x = L is $V(L) - V(0) = \int_0^L E(x)dx = \frac{1}{2} RsJ_BL^2$, where $Rs = \rho/t$ is the ITO sheet resistance.[19] For typical ITO sheet resistance R_S of 10 Ω/□ and vertical current density J_B of 10 mA/cm^2, the voltage

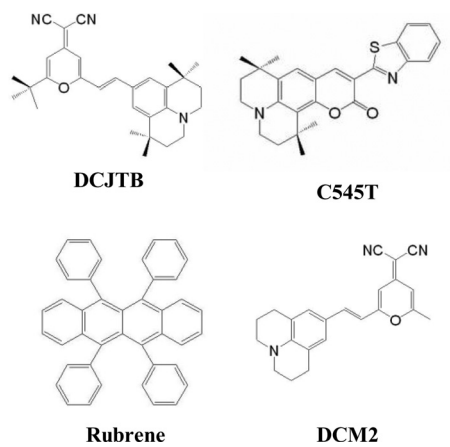

FIG. 30. The molecular structures of DCJTB, C545T, Rubrene, and DCM2.

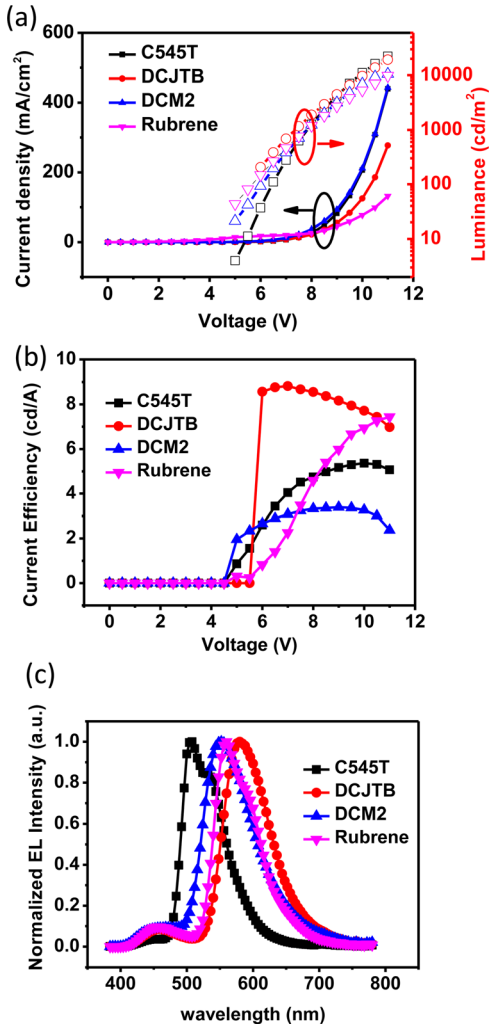

FIG. 31. (Color online) (a) The current density, the luminance, (b) the current efficiency, and (c) the spectrum of the devices with different guest materials.

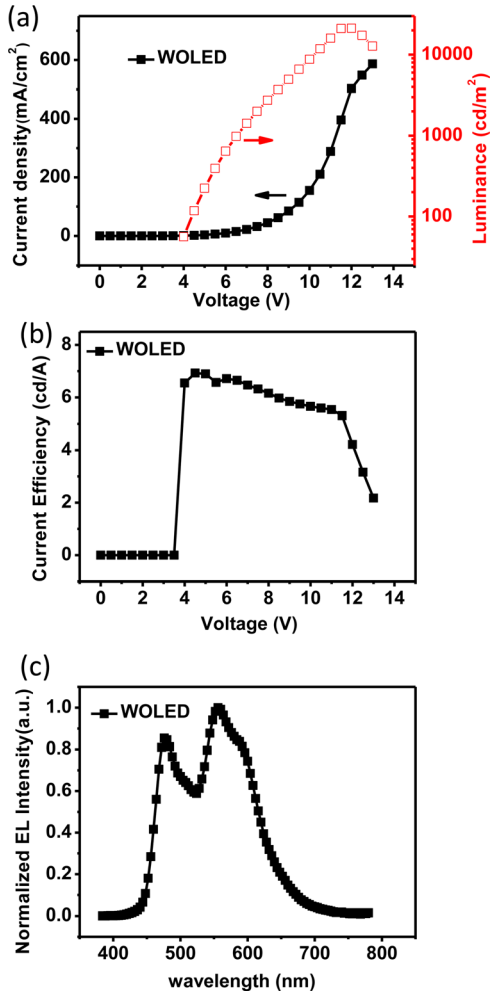

FIG. 32. (Color online) (a) The current density, the luminance, (b) the current efficiency, and (c) the spectrum of the white fluorescence device. The ratio of Blue S, Blue D, and Rubrene is 100:2.36:0.236.

drop across L = 3 cm is 0.45 V. The luminance variance of such voltage drop is hardly visible. However, for L = 5 cm, the voltage drop becomes 1.25 V which is enough to cause visible luminance variation. In case the semiconductor layers are coated for size over 10 cm, the ITO and cathode need to

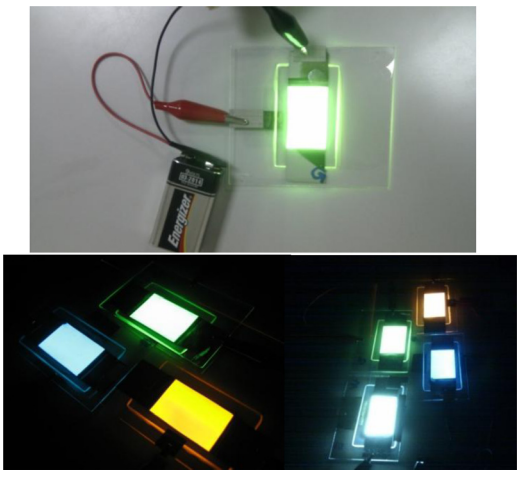

FIG. 33. (Color online) The pictures of large area OLED made by the blade-only method. The active area is 2×3 cm^2.

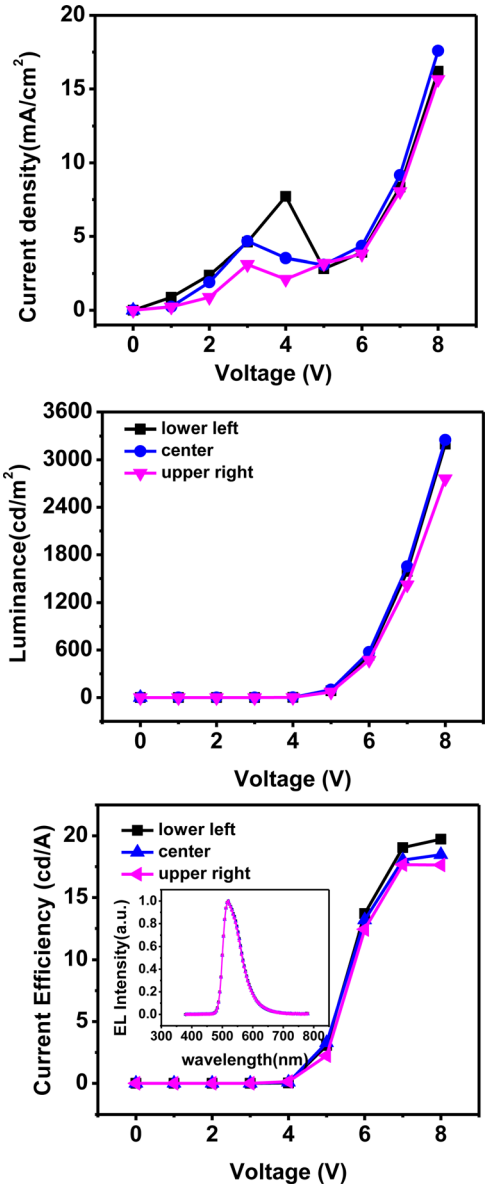

FIG. 34. (Color online) (a) The current density, (b) the luminance, and (c) the current efficiency of the large area green phosphorescence OLED. The inset in (c) shows the spectrum of the device.

be patterned such that the active regions are separated 5 cm by 5 cm blocks for uniformity at high luminance.

E. Solar cell

In addition to OLED, blade coating can also be used for organic solar cell. Unlike OLED, only one single semiconductor layer is needed to achieve high solar power conversion efficiency in the bulk hetero-junction organic solar cell, where the active layer is a blend of an electron donor material and an electron acceptor material. The photon is absorbed by the donor to create an exciton. The exciton is then dissociated at the donor-acceptor interface to yield an electron in the donor and hole in the acceptor. The electrons and holes are transported through the random network of donor and acceptor, respectively, in the bulk hetero-junction to reach the collecting electrode. Phase separation of the donor and acceptor materials in the 10 nm scale is necessary to

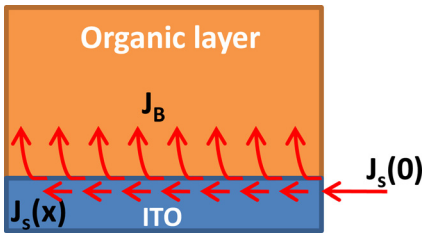

FIG. 35. (Color online) The schematic diagram of current flow from ITO into the device.

form the optimal interpenetrating connected random networks for the exciton dissociation and carrier transport. Good conversion efficiency has been achieved with polymer donor and fullerene derivative by spin coating with high boiling point solvent like dichlorobenzene.[20] The reason for high boiling point is to allow a slow drying of the active layer and enough time or the donor and acceptor molecules to form the desired phase separation. Such approach is called solvent annealing. The slow evaporation, however, takes time and reduces the production efficiency. Furthermore, spin coating wastes most of the materials and is incompatible with the potential roll-to-roll process. Blade coating offers solutions for these problems of spin coating even when only one single active layer is needed.

The common donor polymer poly(3-hexylthiophene-2,5-diyl) (P3HT) and acceptor [6,6]-phenyl-C61-butyric acid methyl ester (PCBM) shown in Fig. 36 are blended in chlorobenzene solution for blade-only coating. PEDOT:PSS is deposited by spin coating. P3HT and PCBM are dissolved in chlorobenzene solution with the concentration 17 mg for each in 1 ml. The blade-only is done with blade gap of 60 μm, hot plate temperature of 100 °C followed hot wind, solution delivery of 23 μl drop. After blade coating, the film is annealed at 140 °C in nitrogen for 20 min. The thickness is 260 nm. Ca of 35 nm and Al of 100 nm are subsequently evaporated to form the top electrode. Large-area uniform film with optimal thickness around 250 nm is obtained by blade coating on hot plate at 100 °C and hot wind from the top as in the case of OLED. Now, there is no need to prevent dissolution by rapid drying. However, rapid drying is necessary to achieve high uniformity at large area by inhibiting reflow of the liquid during drying. Indeed slight variation of

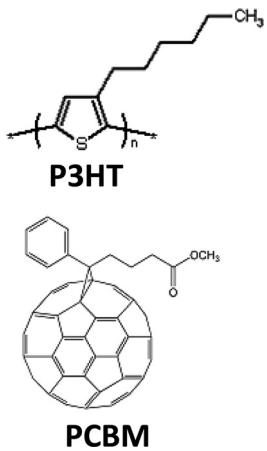

FIG. 36. The molecular structures of the P3HT and the PCBM.

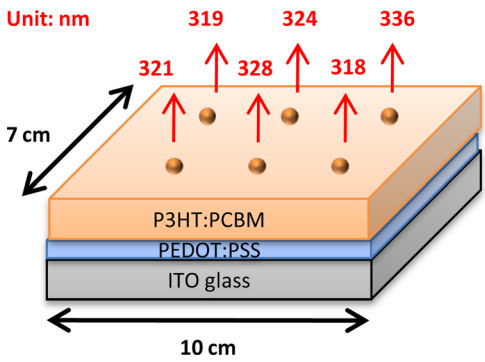

FIG. 37. (Color online) The thickness distribution of a large-area P3HT:PCBM film made by blade-only method.

the substrate temperature may cause gradient of solvent evaporation rate, which in turn cause concentration variation and unpredictable flow of the solid content during drying. Immediate solvent removal by the simultaneous action of bottom substrate heating and top hot wind fixed the solute at where they are deposited initially. Similar situation occurs in the PEDOT:PSS coating for which there is no dissolution concern either. Bottom heating and top hot wind are still required to form a large uniform PEDOT:PSS film. The thickness distribution for large-area P3HT:PCBM film by blade-only method is shown in Fig. 37 for a range of 10 cm. The high uniformity demonstrates the potential of blade-only method for the roll-to-roll production of organic solar cell.

The device characteristics with active area of 2 mm by 2 mm are shown in Fig. 38 for P3HT:PCBM solar cell deposited by blade-only method. Power conversion efficiency of 4.1% is achieved, close to the efficiency of the device by spin coating followed by the slow solvent annealing for about 30 min in dichlorobenzene. Note that in blade-only coating, there is no long drying time. The nano-scale phase separation is able to form within a few seconds of rapid drying. The same power conversion efficiency of device by blade-only suggests that the without the spinning it is easy for the phase separation to form. One possible explanation is that in spin coating, the centrifugal force tends to mix the donor and acceptor and eliminate the phase separation, so it has to take place in the solvent annealing time. On the other hand, in blade-only coating, there is no centrifugal force and the phase separation occurs quickly during the short drying time. Atomic force microscope (AFM) images for the blade-

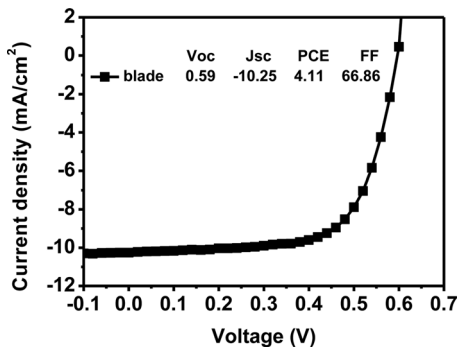

FIG. 38. The current density–voltage (J–V) relations of the organic solar cell made by the blade-only method.

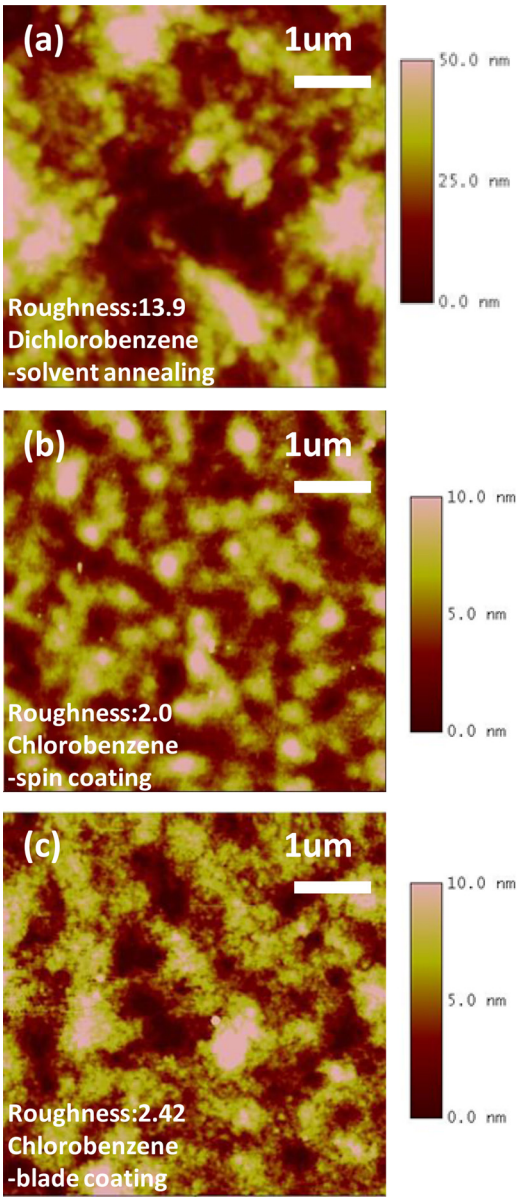

FIG. 39. (Color online) The AFM images of the P3HT:PCBM film made by (a) spin coating with dichlorobenzene solvent annealing, (b) spin coating from chlorobenzene solution, (c) blade-only from chlorobenzene solution.

coated film and spin-coated films are compared in Fig. 39. The roughnesses of the films prepared by blade coating, spin coating, and spin coating followed by solvent annealing in dichlorobenzene are 2.4, 2.0, and 13.9 nm, respectively. The roughness of the blade-coated film is slightly higher than the spin-coated film, but it is lower than the dichlorobenzene solvent-annealed film for a large extent. Although the efficiency of the device with higher roughness is usually superior to the one of the device with lower roughness, the efficiency of the blade-coated device is still compatible to the solvent-annealed device as shown in Fig. 38.

V. CONCLUSION

A continuous coating technique termed blade-only coating method is developed to fabricate multi-layers of organic semiconductor films without dissolution. Immediate drying of the wet film after blade motion is ensured by bottom heating as well as top hot wind. This method works for large area, has low material waste, has high production throughput, and is compatible with roll-to-roll process. The blade-only method is successfully applied to a wide range of multi-layer structures for organic light-emitting diode involving hole transport, emissive, and electron transport layers. This method can be used for conjugated polymers and small molecules. Only marginal solubility of the organic molecules is required for such coating. Multi-layer OLED made by such continuous blade-only method has high efficiency close to the ones made by vacuum deposition. Large-area OLED shows high luminance uniformity and has about the same characteristics as the small-area devices. Very-low-cost production of large-area and high-efficiency OLED lighting is realized by this coating method. The blade-only method is also successfully applied to organic solar cell and yield the same efficiency as spin-coated devices, making possible low-cost roll-to-roll production of organic solar cells. The blade-only method has general applicability to a wide range of organic semiconductors regardless of the molecular weight. The method is ready for large-scale industrial production of all opto-electronic and electronic products based on organic semiconductors.

ACKNOWLEDGMENTS

This work is supported by the National Science Council of Taiwan under Contract No. 99-2628-M-009-001 and the Ministry of Economic Affairs of Taiwan under Contract No. 99-EC-17-A-07-S1-157.

[1]H. Wang, K. P. Klubek, and C. W. Tang, Appl. Phys. Lett. **93**, 093306 (2008).
[2]H. Jiang, Y. Zhou, B. S. Ooi, Y. Chen, T. Wee, Y. L. Lam, J. Huang, and S. Liu, Thin Solid Films **363**, 25 (2000).
[3]D. Liu, C. G. Zhen, X. S. Wang, D. C. Zou, B. W. Zhang, and Y. Cao, Synth. Met. **146**, 85 (2004).
[4]R. J. Holmes, S. R. Forrest, Y. J. Tung, R. C. Kwong, J. J. Brown, S. Garon, and M. E. Thompson, Appl. Phys. Lett. **82**, 2422 (2003).
[5]S. F. Chen and C. W. Wang, Appl. Phys. Lett. **85**, 765 (2004).
[6]J. Li, C. Ma, J. Tang, C. S. Lee, and S. Lee, Chem. Mater. **17**, 615 (2005).
[7]M. T. Chu, M. T. Lee, C. H. Chen, and M. R. Tseng, Org. Electron. **10**, 1158 (2009).
[8]G. He, M. Pfeiffer, K. Leo, M. Hofmann, J. Birnstock, R. Pudzich, and J. Salbeck, Appl. Phys. Lett. **85**, 3911 (2004).
[9]S. Reineke, F. Lindner, G. Schwartz, N. Seidler, K. Walzer, B. Lüssem, and K. Leo, *Nature* **459**, 234 (2009).
[10]S. R. Tseng, H. F. Meng, K. C Lee, and S. F Horng, Appl. Phys. Lett. **93**, 153308 (2008).
[11]J. D. You, S. R. Tseng, H. F. Meng, F. W. Yen, I. F Lin, and S. F. Horng, Org. Electron. **10**, 1610 (2009).
[12]L. C. Ko, Z. Y. Liu, C. Y. Chen, C. L. Yeh, S. R. Tseng, H. F. Meng, S. C. Lo, P. L. Burn, and S. F. Horng, Org. Electron. **11**, 1005 (2010).
[13]Z. Y. Liu, S. R. Tseng, Y. C. Chao, C. Y. Chen, H. F. Meng, S. F. Horng, Y. H. Wu, and S. H. Chen, Synth. Met. **161**, 426 (2011).
[14]S.Y. Huang, H. F. Meng, H. L. Huang, T. C. Chao, M. R. Tseng, Y. C. Chao, and S.F. Horng, Synth. Met. **160**, 2093 (2010).
[15]Y. C. Chao, S. Y. Huang, C. Y. Chen, Y. F. Chang, H. F. Meng, F. W. Yen, I. F. Lin, H. W. Zan, and S. F. Horng, Synth. Met. **161**, 148 (2011).
[16]S.-J. Su, T. Chiba, T. Takeda, and J. Kido, Adv. Mater. **20**, 2125 (2008).
[17]J. Lee, N. Chopra, S. H. Eom, Y. Zheng, J. Xue, F. So, and J. Shi, Appl. Phys. Lett. **93**, 123306 (2008).
[18]X. H. Yang, F. Jaiser, S. Klinger, and D. Neher, Appl. Phys. Lett. **88**, 021107 (2006).
[19]A. K. Pandey, J. M. Nunzi, B. Ratier, and A. Moliton, Phys. Lett. A **372**, 1333 (2008).
[20]G. Li, Y. Yao, H. Yang, V. Shrotriya, G. Yang, and Y. Yang, Adv. Funct. Mater. **17**, 1636 (2007).